Hindawi
Journal of Food Biochemistry
Volume 2024, Article ID 4822900, 14 pages
https://doi.org/10.1155/2024/4822900

Research Article

In Vivo and *In Vitro* Study on the Mechanism of Anticervical Cancer Effects of Corilagin in Mice

Li-Mei Wang,[1] **Yu-Han Jiang**,[1] **Xing-Yu Li**,[1] **Min-Rui Wu**,[1] **Zi-Yang Xu**,[1] **Long-Jie Li**,[1] **Yang Yi**,[2] **and Hong-Xun Wang**[1]

[1]*School of Life Science and Technology, Wuhan Polytechnic University, Wuhan 430023, China*
[2]*School of Food Science and Engineering, Wuhan Polytechnic University, Wuhan 430023, China*

Correspondence should be addressed to Hong-Xun Wang; wanghongxun7736@163.com

Received 6 March 2024; Revised 23 April 2024; Accepted 3 May 2024; Published 13 May 2024

Academic Editor: Ignazio Restivo

Background. Corilagin has several pharmacological effects such as antitumor, anti-inflammatory, and cardiovascular disease treatment. Our previous studies have shown that the Corilagin can significantly inhibit proliferation of HeLa cells. However, there are no scientific data on the anticervical cancer effect of Corilagin *in vivo*. *Methods*. Network pharmacology was used to predict the mechanism, followed by *in vitro* experiments to detect cell proliferation, cycle, and apoptosis, and *in vivo* experiments to verify the mechanism. *Results*. It was speculated that the mechanism of action for the anticervical cancer of Corilagin could be related to PI3K/AKT and MAPK signaling pathways through network pharmacology. Results of cell assays in the present study showed that the Corilagin has significant effect on the proliferation, cell cycle, and apoptosis of murine cervical cancer U14 cells *in vitro*. In addition, Corilagin can significantly inhibit the growth of U14 tumor-bearing mice with insignificant toxic effect on the liver and kidney of the transplanted mice. The current study found that Corilagin can delay development of cervical cancer by boosting antitumor immune responses of the body. RT-PCR and Western blotting were applied in the current study to evident that Corilagin can achieve anticervical cancer property by inducing apoptosis of tumor tissues through both PI3K/AKT and MAPK signaling pathways. *Conclusion*. Therefore, this study provided theoretical reference for research of Corilagin as a bioresource for development of an anticervical cancer drug and functional food.

1. Introduction

Cervical cancer is a malignant tumor that occurs at the junction of squamous epithelial cells in cervical vagina. It can also infect the transition zone and columnar epithelial cells in the inner lining of the neck tube. Globally, cervical cancer is the fourth most common cancer and the fourth leading causes of cancer deaths among women. In 2018, there were 570,000 patients with cervical cancer and 311,000 reported deaths from the cancer in the world [1–3]. Surgical operation together with radiotherapy and chemotherapy are the common methods of cervical cancer treatment. However, the strategies do not effectively eradicate the tumor tissue in patients with locally advanced, recurrent, and metastatic cervical cancer. In terms of chemotherapeutic drug selection, 5-fluorouracil (5-FU) has been used for many years as an anticervical cancer drug for optimal postoperative survival, but recently frequent emergence of drug resistance has limited the clinical use of 5-FU [4], and there is an urgent need for treatment methods that are both effective and low toxic. This shall improve the outcome of cervical cancer treatment and reduce the mortality rate of patients with the cancer.

Corilagin is a type of ellagitannin which is a natural component in several ethnopharmacological plants. Its chemical formula and molecular weight are $C_{27}H_{22}O_{18}$ and 634.45, respectively. It is an off-white needle-like crystalline powder which is soluble in methanol, ethanol, acetone, and dimethyl sulfoxide. To date, Corilagin has been detected in 50 species of 16 plants families [5]. The ellagitannin is one of the main active ingredients of various ethnic medicines, such as *Phyllanthus urinaria* [6], matsumura leaf flower herb [7],

and *Euryale ferox* Salisb. seed [8]. Recent pharmacological studies have found that Corilagin has antitumor [9], anti-inflammatory [10], antibacterial [11], and antiviral [6] effects. It has significant application prospects especially in the antitumor pharmacological aspect. Currently, there is no *in vivo* study of Corilagin against cervical cancer.

Results of our preliminary studies found that Corilagin isolated from the shell of the *Euryale ferox* Salisb. seed has a significant inhibitory effect on proliferation, migration, and invasion of cervical cancer HeLa cells. This indicates that ellagitannin has enormous potential in combating cancer [12]. Therefore, the current study started from investigation of the chemical structure of Corilagin. The study later applied the network pharmacology technology to predict its antitumor target genes and their mechanisms. Experiments were conducted on the effects of Corilagin on U14 cell proliferation, cell cycle, and apoptosis. Finally, its antitumor effect and molecular mechanism were studied by establishing a subcutaneous xenograft model of cervical cancer in mice to investigate the effect of Corilagin on the growth of xenograft.

2. Materials and Methods

2.1. Materials and Reagents. Cervical cancer U14 cells were acquired from iCell Bioscience Inc. (Shanghai, China), Corilagin (purity ≥98%): Chengdu Chroma-Biotechnology Co. Ltd. (Chengdu, China), phosphate buffered saline solution (PBS), and Dulbecco's modified eagle medium (DMEM; Gibco, America); female Kunming mice aged 4–6 weeks were purchased from Hubei Provincial Center for Disease Control and Prevention (Qualified number: SCXK2020-0018); 5-FU: Sigma-Aldrich in America; trypsin cell digestion solution: Biosharp Biotechnology Co., Ltd. (Hefei, China); fetal bovine serum (FBS): Hangzhou Sijiqing Bioengineering Company (China); CCK-8 kit: Tongren Company in Japan; DNA content (cell cycle) detection kit: Solabao Technology Co., Ltd. in Beijing, China; apoptosis double stain detection kit: Bestbio in Shanghai, China; TNF-α kit, IL-2 kit, and IL-10 kit: Beijing 4A Biotech Co. Ltd. (China); RNAiso Plus reagents, RNA reverse transcription kits, and real-time fluorescent quantitative RT-PCR kits: Takara Company in Japan; mouse monoclonal antibody β-actin (42 KDa): Aibotech (Wuhan, China); rabbit anti-EGFR (130 KDa), rabbit anti-Beclin 1 (50 KDa), and rabbit anti-P-AKT308 (56 KDa): Bioss in Beijing, China; rabbit anti-JNK (50 KDa), rabbit anti-AMPK (63 KDa), and rabbit anti-AKT (56 KDa): Proteintech Group, Inc. in Wuhan China; mouse anti-Caspase 9 (49 KDa): Cell Signaling Technology, Inc. (CST, America); Ggoat antimouse IgG (H + L) HRP and goat antirabbit IgG (H + L) HRP: Jackson Immuno Research Laboratories Inc. (America); microscope: Olympus Corporation (Japan).

2.2. Prediction of Potential Target Genes for Anticervical Cancer Effect of Corilagin. First, the secondary chemical structure of Corilagin was searched in the TCMSP database. The PharmMapper and SwissTargetPrediction were then used to predict the target that can bind Corilagin. The related genes of cervical cancer were screened using GeneCards, OMIM, and DisGeNET databases to establish a cervical cancer target database. The intersection with the above targets was the potential target of Corilagin's anticervical cancer.

2.3. Construction of Potential Target Interaction Networks for the Anticervical Cancer Effect of Corilagin. The potential targets obtained in Section 2.2 of this study were used to construct the PPI network map using the STRING database. The targets that did not interact with other proteins were deleted and the derived data were used to make a protein interaction map using Cytoscape_v3.6.1.

2.4. Establishment of a Pathway Network for the Potential Anticervical Cancer Target of Corilagin. The targets obtained in Section 2.2 were uploaded in the DAVID database. The KEGG pathway enrichment analysis was performed to investigate the anticervical cancer targets of Corilagin.

2.5. Detection of Cell Proliferation Inhibition Rate. The cells in the logarithmic growth phase were counted and laid according to 3,000 cells/well. The concentration of Corilagin and 5-FU was set at 0, 200, 400, 600, 800, and 1000 μmol/L. The treatment time were set at 24 h and 48 h. The OD values were then assayed according to the growth manipulation instructions provided with the CCK-8 kit, and the cell proliferation inhibition rate was calculated according to formula (1). The ODtest group represents the OD of the group with cells but without drug administration; the ODblankgroup represents the OD of the drug-free and cell-free group; the ODcontrol group represents the OD of the administered group.

$$\text{Inhibition rate of cell proliferation}\,(\%) = 1 - \frac{(\text{ODtest group} - \text{ODblank group})}{(\text{ODcontrol group} - \text{ODblank group})} \times 100\%. \quad (1)$$

2.6. Detection of Cell Cycle. 5×10^5 cells/well were seeded into a 6-well plate. After the cells adhered to the wall, they were treated with different concentrations of Corilagin (0, 200, 400, 600, 800, and1000 μmol/L). After 48 h, the cells were processed according to the procedure provided in the kit and detected the apoptosis by flow cytometry.

2.7. Detection of Apoptosis. 5×10^5 cells/well were plated into a 6-well plate. After the cells adhered to the wall, they were treated with different concentrations of Corilagin (0, 200, 400, 600, 800, and 1000 μmol/L). After 48 h, the cells were processed according to the procedure described in the kit and then detected the apoptosis by flow cytometry.

2.8. Detection of Transplanted Tumors' Growth and Tumor Tissue Apoptosis. The mice were randomly divided into 5 groups, each with similar body weight, with 10 mice in each group. Tumor cells were subcultured in mouse ascites for three times, and the cell suspension was then prepared with sterile PBS at a concentration of 1×10^7/ml. In addition to the blank group, subcutaneous injection was performed in the right axillary and at the dose of 0.2 ml per mouse (2×10^6 cells per mouse). Vaccination had a 100% success rate. The blank and negative control groups were each time intraperitoneally injected with 0.2 ml PBS, whereas the positive control group was injected with 5-FU (20 mg/kg). The experimental groups were divided into Corilagin high-dose and low-dose groups that were injected with 30 and 15 mg/kg of Corilagin, respectively. The administration of the various treatments began 24 h after subcutaneous injection of tumor cells to the mice. A total of 7 doses were given through intraperitoneal injection every day for 15 consecutive days.

The blood from the eyeballs was taken and the mice were then sacrificed through cervical dislocation. The tumor tissue in the right axilla of mice was carefully isolated and the total mass of the tumor tissue was measured to calculate the tumor inhibition rate by formula (2). Measure and calculate tumor volume by formula (3). The tumor tissues were embedded in paraffin, sectioned, and stained using both TUNEL and H&E.

$$\text{Tumor inhibition rate} = \frac{\text{tumor weight in model group} - \text{tumor weight in the treatment group}}{\text{tumor weight in model group}} \times 100\%, \tag{2}$$

$$\text{Tumor volum} = \frac{\text{long} \times \text{width}^2}{2}. \tag{3}$$

2.9. Organ Coefficients' Calculation and H&E Staining Analysis. The livers and kidneys of mice were dissected, weighed to calculate organ coefficients, and organs were sectioned and stained with H&E. They were then examined microscopically to see if the drug had damaged their tissues.

2.10. ELISA: Detection of IL-2, TNF-α, and IL-10 Indicators in Serum. After 30 min of indoor coagulation, the levels of IL-2, TNF-α and IL-10 in the serum were detected through centrifugation at 1000 g for 10 min according to the procedure described on the ELISA kit.

2.11. RT-PCR: Detection of the mRNA Expression. Based on the results of the previous experiments, the group with the best results was selected for the experiment. The RNA of the tumor tissue was extracted through the Trizol method and reverse transcription was then performed. The cDNA obtained was stained with SYBR and then subjected to the real-time fluorescence quantitative analysis through a two-step procedure. The amplification procedure included an initial incubation at 60°C for 30 s, followed by incubation at 95°C for 3 s, and then 40 cycles in a sequence.

2.12. Western Blot Detection of Protein Expression. The tissues were collected from the high-dose group and the model group. The weighed tumor tissue was placed in EP tubes and their protein was quantified using the BCA kit. Protein supernatant was prepared with buffer at the ratio of 4 : 1(buffer: protein supernatant) and then added to the protein sample. The protein can be stored in the chain form for 10 min at temperature between 80 and 95°C.

The protein samples were injected into the sample pool of the gel preparation instrument and then added into the separation gel sample wells for separation through electrophoresis. The gels were cut according to the position of protein markers, and the membranes were transferred at 100 V for 90 min in an ice-cold water bath. The membrane was cleaned thrice with TBST for 5 min each time. The first antibody was added and incubated overnight at 4°C. The primary antibody was washed three times with TBST. The second antibody was then added and incubated at room temperature for about 1 h. The second antibody was finally washed three times with TBST. After adding the developer, the images were scanned using a gel imager and analyzed using the Image J analysis software.

2.13. Statistical Analysis. GraphPad Prism 8.0.1 was used to plot graph for the obtained data and analyzed the significant difference. The results are expressed as mean ± standard deviation (mean ± SD) and the difference between groups was tested using *t* tests. Statistically significant difference was set as $p < 0.05$.

3. Results

3.1. Potential Target Genes for the Anticervical Cancer of Corilagin. Through the drug structure (Figure 1(a)), the present study used the Uniprot database to screen out 334 target genes that can be combined with Corilagin. A total of 7,076 genes related to cervical cancer were screened using GeneCards, OMIM, and DisGeNET databases. Both databases (OMIM and DisGeNET) drew the Venn diagram as presented in Figure 1(b), which shows that there were 222 common target genes.

3.2. Protein Interaction Network Analysis. The protein interaction data of the potential target genes were obtained from the STRING database and the data were imported into Cytoscape to construct the "protein interaction" network diagram (Figure 2). The color was set based on the degree value. The larger the degree value, the darker the color and the higher the correlation with other targets; *MAPK1, SRC, PIK3R1, TP53, HSP90AA1, HRAS, RHOA*, and other important genes were screened.

The 31 key targets with high degree values were screened to be visible in the tumor signaling pathway by the KEGG Mapper function in the KEGG database. According to Figure S1, we found that the selected targets include BCL-2, BCL XL, CASPASE3, and other related apoptotic targets. Furthermore, it was noted that the selected targets mainly function through PI3K/AKT pathway and MAPK signaling pathway. This indicates that Corilagin may affect the PI3K/AKT and MAPK signaling pathways to cause tumor apoptosis and achieve the anticervical cancer effect.

3.3. KEGG Enrichment Pathway Analysis. The KEGG enrichment analysis was carried out on the relevant target genes using the DAVID database. A total of 105 significantly enriched signal pathways were screened out, broad pathways were excluded, and 17 more significant pathways were finally obtained (Figure 3). It was evident that the pathways with larger enrichment factors and a larger number of counts under the pathway include PI3K-AKT, RAS, RAP1, MAPK, FOXO, and HIF-1 signaling pathways.

RAS protein is a type of small GTPases superfamily which is composed of KRAS, HRAS, and NRAS. It plays a regulatory role in the growth of many normal cells. Missense mutations in the *RAS* gene have been found in 25% of human cancers. The gene makes the research on the treatment of cancer by inhibiting the *RAS* gene become a hot spot. RAS binds to a variety of effector proteins and hence can transmit downstream signals to control cell proliferation, differentiation, adhesion, migration, and survival. Research studies on the targeted RAS focuses on inhibition of downstream signaling pathways because it is difficult to directly target the small molecular mutant RAS. The RAS sends signals through a variety of effectors. The signals mainly stimulate both the MAPK and PI3K/AKT pathways [13]. Furthermore, RAP1 has a high degree of sequence similarity with RAS and it is a member of the RAS family of small GTPases. The RAP1 has overlapping binding partners. Mechanistically, RAS and RAP1 cooperate to initiate and maintain ERK signaling. RAP1 can also be directly combined with the RAS binding domain that stimulates PI3K [14]. This shows that both RAS and RAP1 signaling pathways can play a significant role in influencing the MAPK and PI3K/AKT pathways. In conclusion, it was evident that the mechanism of Corilagin against cervical cancer may be related to PI3K/AKT and MAPK signaling pathways.

3.4. Inhibition of Cell Proliferation in U14 Cervical Cancer. The effect of Corilagin on proliferation of U14 cells was assessed after Corilagin was allowed to act on the cells for 24 h or 48 h. Results of the analysis are as presented in Figure 4. It was evident that Corilagin has a significant inhibitory effect on the proliferation of U14 cells. It was found that Corilagin at a concentration of 200 μmol/L showed proliferation inhibition of U14 cells after 24 h or 48 h, with inhibition rates of 1.51% and 1.64%, respectively, which were lower than that of the positive drug (5-FU).

At the concentration of 400 μmol/L, Corilagin showed a higher inhibitory effect as compared with that at concentration of 200 μmol/L. The inhibition rate of Corilagin (400 μmol/L) on U14 cell proliferation at 24 h and 48 h was $64.72 \pm 6.05\%$ and $75.18 \pm 7.74\%$, respectively, which were higher than the inhibitory effect of 5-FU (positive control group). The inhibitory effect of Corilagin at concentrations higher than 400 μmol/L was higher than that of 5-FU. Furthermore, its IC_{50} value after 24 h and 48 h exposure to the U14 cell was 372.4 μmol/L and 394.5 μmol/L, respectively (Supplement materials Table S2).

3.5. Effects of Corilagin on U14 Cell Cycle. Results of the present study showed that the number of cells in the G0/G1 phase remained basically unchanged as compared with that in the model group after Corilagin was applied to U14 cells for 48 h, at concentrations lower than 400 μmol/L (Figure 5). Furthermore, it was noted that the number of cells in S phase increased, whereas that in the G2/M phase was reduced as compared with that in the control group after drug exposure to the cells for 48 h at drug concentrations lower than 400 μmol/L.

On the other hand, when the concentration of Corilagin was higher than 400 μmol/L, it was found that the number of cells in the G0/G1 phase increased in concentration-dependent manner. However, the number of cells both in the S and G2/M phases significantly decreased as compared with the control (model) group. This showed that reduced concentrations of Corilagin (below 400 μmol/L) blocked proliferation of U14 cells in the S phase, whereas higher concentration (above 400 μmol/L) blocked proliferation of the cells in the G0/G1 phase.

Progression of the cell cycle is maintained by a variety of molecules such as growth factors and hormones. It also involves a series of strictly regulated molecular processes that ultimately causes cell division. The cell cycle includes four stages: G1 (premitosis), S (DNA replication), G2 (mitosis preparation), and M (genetic material and

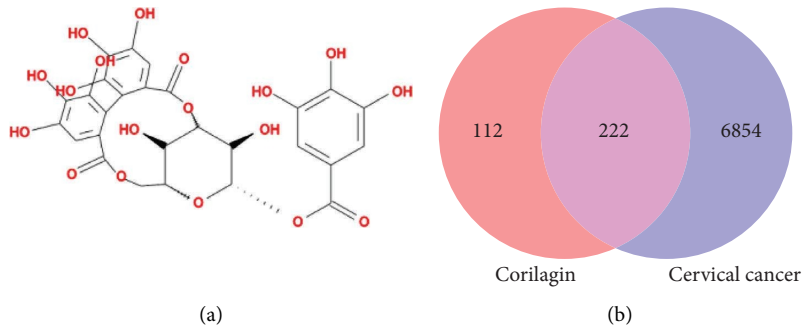

Figure 1: (a) The structural formula of Corilagin. (b) Venn diagram showing the Corilagin-disease interactions.

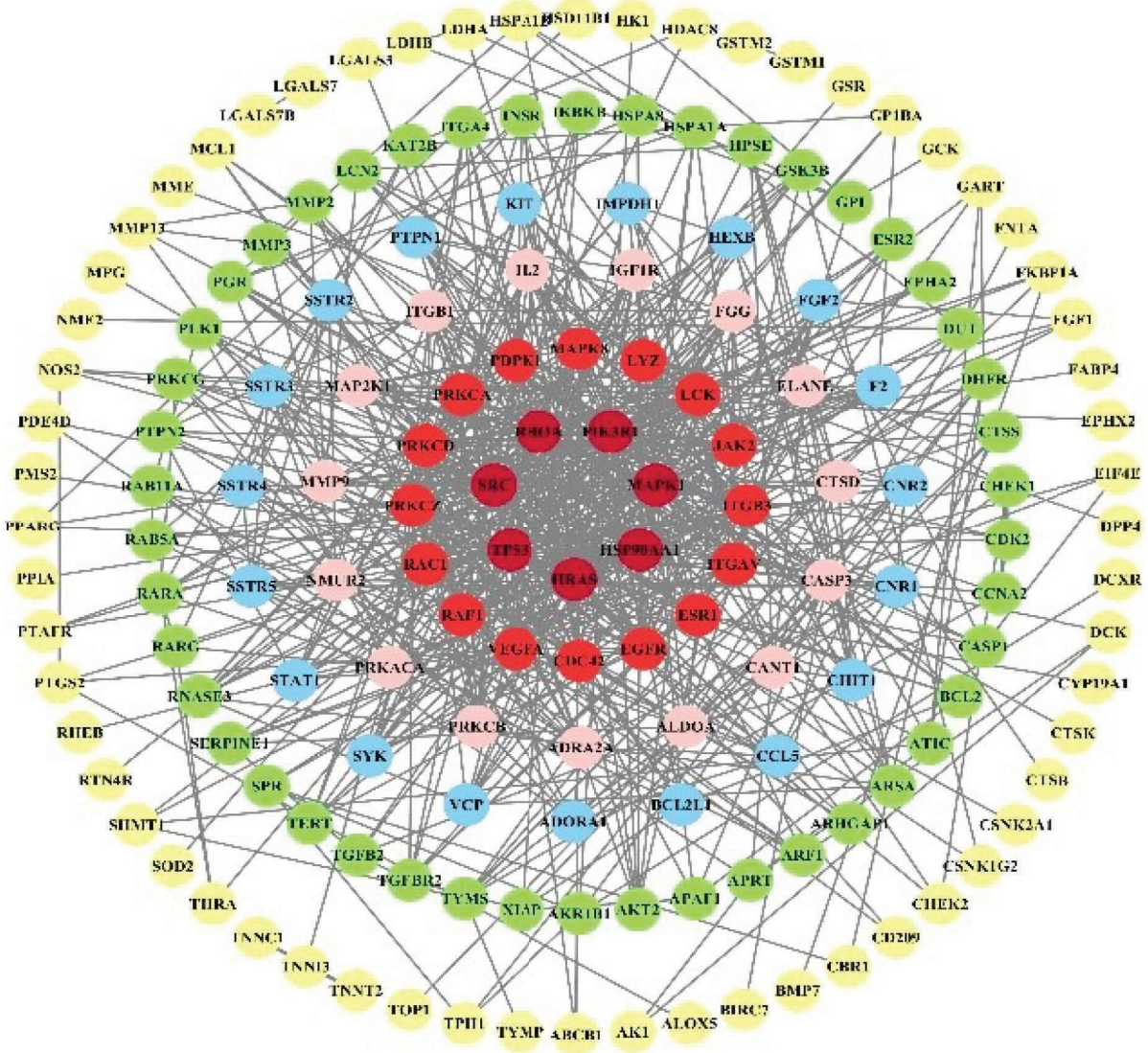

Figure 2: Protein interaction network diagram of potential targets. Protein interaction network diagram: the higher the degree value, the darker the color.

cytokinesis). Dysregulation of the cell cycle is the cause of abnormal cell proliferation and cancer [15]. Previous studies have shown that Corilagin can affect the cell cycle in the tumor. Furthermore, the drug can block the G2/M phase of liver cancer cells and has been associated with the activation of P53-P21CIP1-CDC2/Cyclin B1 [16].

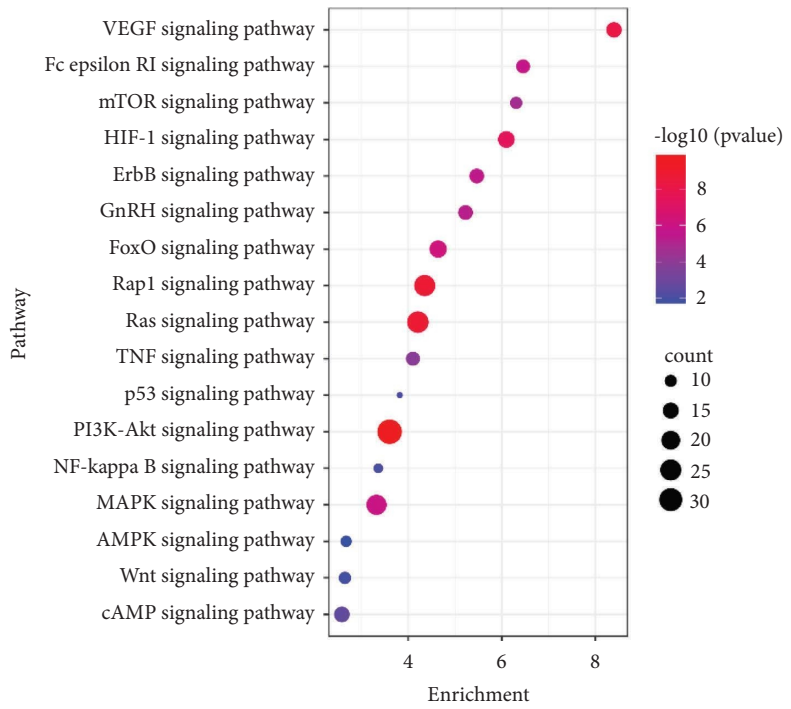

Figure 3: KEGG pathway analysis.

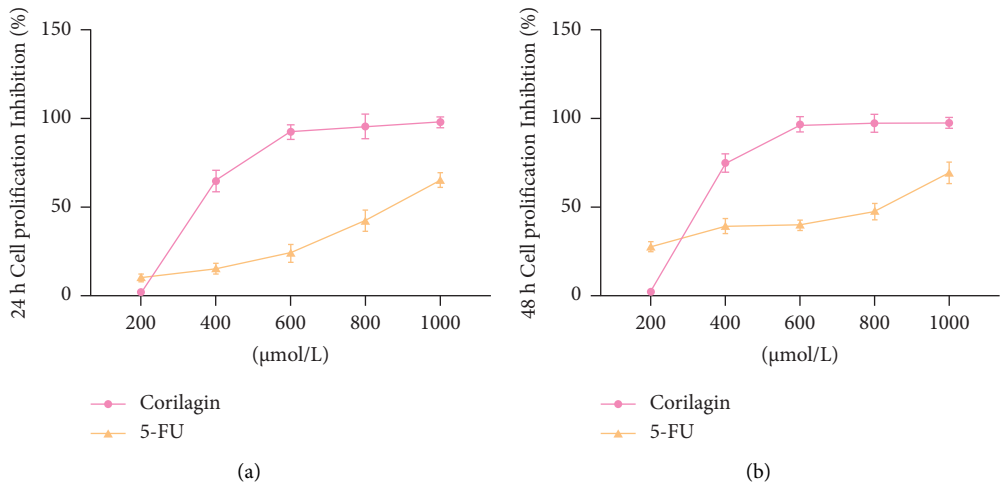

Figure 4: Effect of Corilagin on proliferation of U14 cells. U14 cells were treated with 0, 200, 400, 800, and 1000 μmol/L Corilagin and 5-FU, respectively, for (a) 24 h and (b) 48 h.

3.6. Effects of Corilagin on Apoptosis of U14 Cells. Results of the current study showed that there was an increase in the rate of apoptosis with increase in the concentration of Corilagin as compared with the rate in the control group (Figure 6). For instance, when the drug concentration was 400 μmol/L, the rate of apoptosis was significantly different, whereby the rates for early and late withering cells were $13.6 \pm 3.89\%$ and $35.22 \pm 13.69\%$, respectively. In summary, it was evident that Corilagin has a significant effect on the apoptosis process of the U14 cells.

3.7. Effects of Corilagin on the Growth of Transplanted Tumors and Tumor Tissue Apoptosis in Mice. It was found that both the Corilagin and positive drug (5-FU) groups had different degrees of inhibition on the growth of transplanted tumors in mice (Figure 7). The rate of tumor inhibition by Corilagin in the low-dose group was 43.39%, whereas the tumor volume was reduced by 51.92% as compared with the negative control group. Furthermore, the inhibition effect of Corilagin and 5-FU drugs in the high-dose group was more significant, and the tumor inhibition rates were 53.99% and

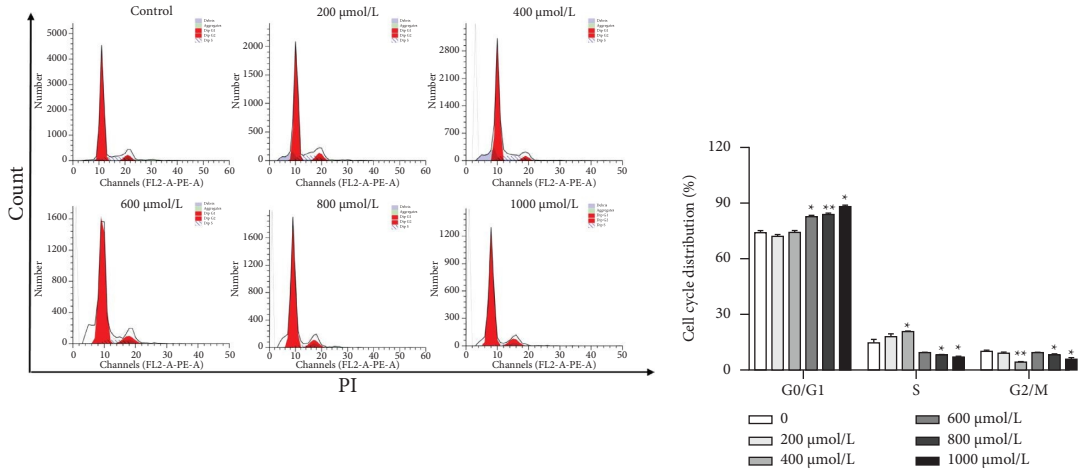

(a) (b)

Figure 5: Effects of Corilagin on U14 cell cycle: (a) the intracellular fluorescence intensity of U14 cells was measured after 48 h of treatment with 0, 200, 400, 800, and 1000 μmol/L Corilagin, respectively. (b) Average fluorescence intensity ($^{*}p < 0.05$ and $^{**}p < 0.01$ vs. 0 μmol/L).

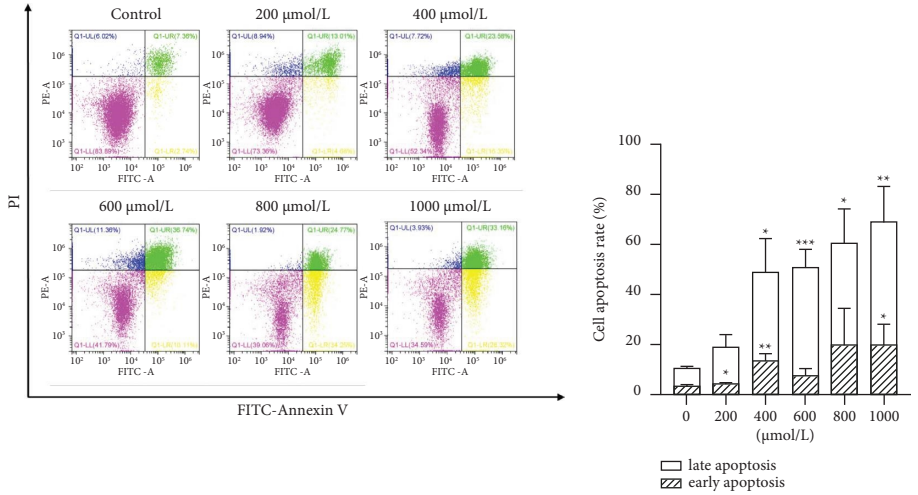

(a) (b)

Figure 6: Effects of Corilagin on apoptosis of U14 cells: (a) the apoptosis rate of U14 cells after 48 h of treatment with 0, 200, 400, 800, and 1000 μmol/L and (b) average apoptosis rate ($^{**}p < 0.01$ and $^{***}p < 0.001$ vs. 0 μmol/L).

54.30%, respectively ($p < 0.05$), whereas the tumor volumes were decreased by 62.92% and 56.70%, respectively ($p < 0.01$) (Supplement Materials Table S3).

This study showed that the tumor tissues in the negative control were mainly normal tumor cells with a small amount of apoptotic cell particles (Figure 8). However, it was evident that both the high-dose Corilagin and the positive drug (5-FU) groups contained a large area of apoptotic cells. The apoptotic area observed in the high-dose Corilagin group was larger than that of the 5-FU group which indicated that Corilagin could more significantly induce tumor tissue apoptosis as compared with the positive drug.

3.8. The Effect of Corilagin on Organ Coefficient and the Histopathology of Mice. Figure 9 shows that the kidney organ coefficients of the model group were comparable with those in the blank group, but the liver organ coefficients ($p < 0.05$) were higher in the model group than in the blank group. This indicates that the liver function of the transplanted tumor mice may decrease and the kidney tissue may not be affected. Notably, between the model group and the drug administration groups, there was no significant difference in the kidney organ coefficients, indicating that neither Corilagin nor 5-FU had a significant effect on the kidney tissue. The organ coefficient of the liver in mice

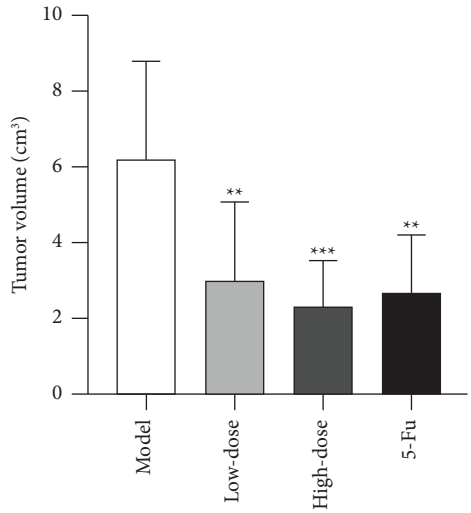

Figure 7: Effects of Corilagin and 5-FU on tumor volume. The effects of Corilagin and 5-FU on tumor volume in mice. The dose was 15 mg/kg in the low-dose group, 30 mg/kg in the high-dose group, and 20 mg/kg in the 5-FU group ($^{**}p < 0.01$ and $^{***}p < 0.001$ vs. 0 mg/kg).

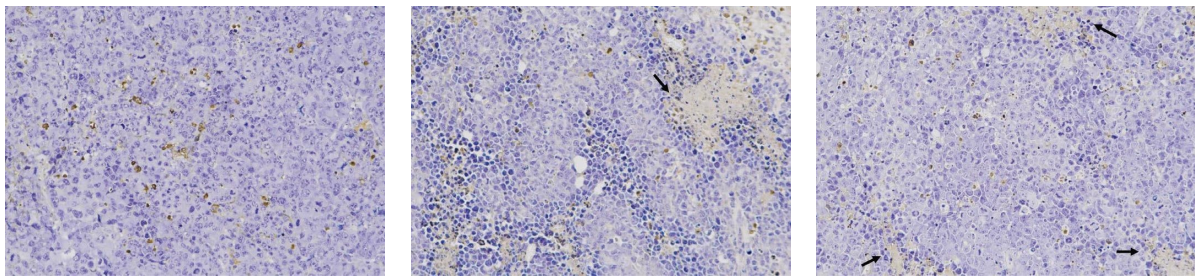

(a) (b) (c)

Figure 8: Effects of the administration group on tumor tissue apoptosis in mice (200x): (a) model group, (b) Corilagin high-dose group, and (c) positive drug group.

treated with high doses of Corilagin decreased significantly ($p < 0.05$), which indicates that high-dose Corilagin may confer protection on the liver function.

Morphological and structural analyses showed that liver cells in the blank group were normal, and the nucleus as well as the cytoplasm were evenly distributed (Figure 10). Except for the blank group, a large amount of hepatocyte edema was seen in the liver tissues of all other groups. This was accompanied by a loose and slightly stained (black arrow) cytoplasm. Neutrophil infiltration (red arrow) was seen around the bile duct in the portal area. Moreover, a few extramedullary hematopoietic foci (yellow arrows) were seen indicating that the liver of the transplanted tumor mice had lesions.

The surface envelope of the kidney tissue is composed of a dense connective tissue with uniform thickness. The kidney parenchyma consists of superficial cortex and deep medulla. According to the pathological observation of kidneys (Figure 11), the cortical medulla of the kidney tissues were clearly demarcated in all groups, the glomeruli were evenly distributed in the cortex, and the number of cells and matrix in the glomeruli were uniform. The renal tubule epithelial cells were round and full, the brush borders were neatly arranged, and the medulla is not significantly damaged. The connective tissue between the urinary tubules forms the interstitial fluid. In this study, the interstitial did not proliferate; and no obvious inflammatory changes were seen.

In summary, the liver of mice transplanted with U14 cells showed severe damage compared with normal mice. The high-dose Corilagin and 5-FU did not significantly alleviate liver damage. Moreover, there was no significant difference in the kidney tissues of the mice across the groups, which indicated that Corilagin and 5-FU had no significant toxic effects on the kidneys, and the results were consistent with the results of organ coefficients. In practice, the liver and kidney functions are jointly monitored, and drugs targeting the liver and kidneys are similar.

3.9. The Effect of Corilagin on IL-2, TNF-α, and IL-10 on Serum Levels in Mice. As shown in Figure 12, mice in the model group had significantly lower serum levels of IL-2 and higher levels of IL-10 than those in the blank group. However, there was no significant difference in the content of TNF-α between the two groups. The levels of IL-2 and TNF-α in the

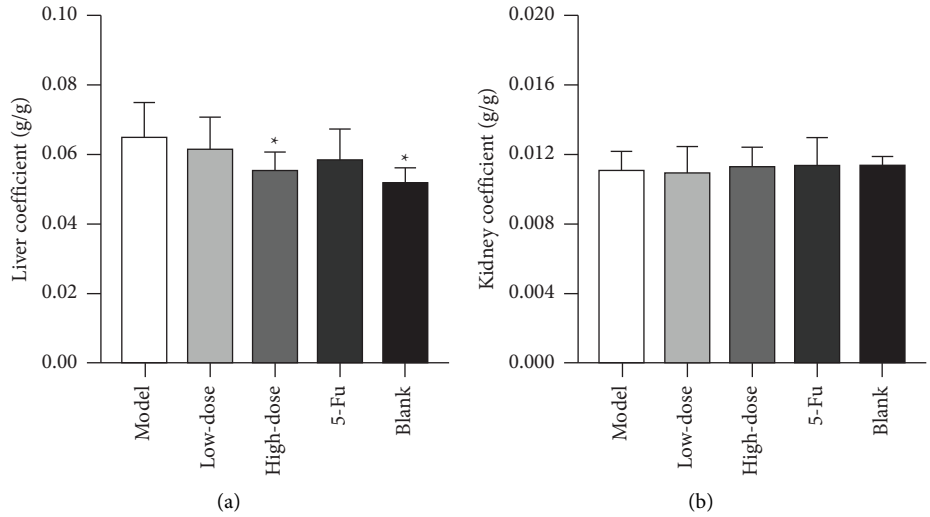

Figure 9: The changes of organ coefficient in mice induced by Corilagin: (a) liver coefficient and (b) kidney coefficient. The dose was 15 mg/kg in the low-dose group, 30 mg/kg in the high-dose group, and 20 mg/kg in the 5-FU group ($^{*}p < 0.05$ vs. 0 mg/kg).

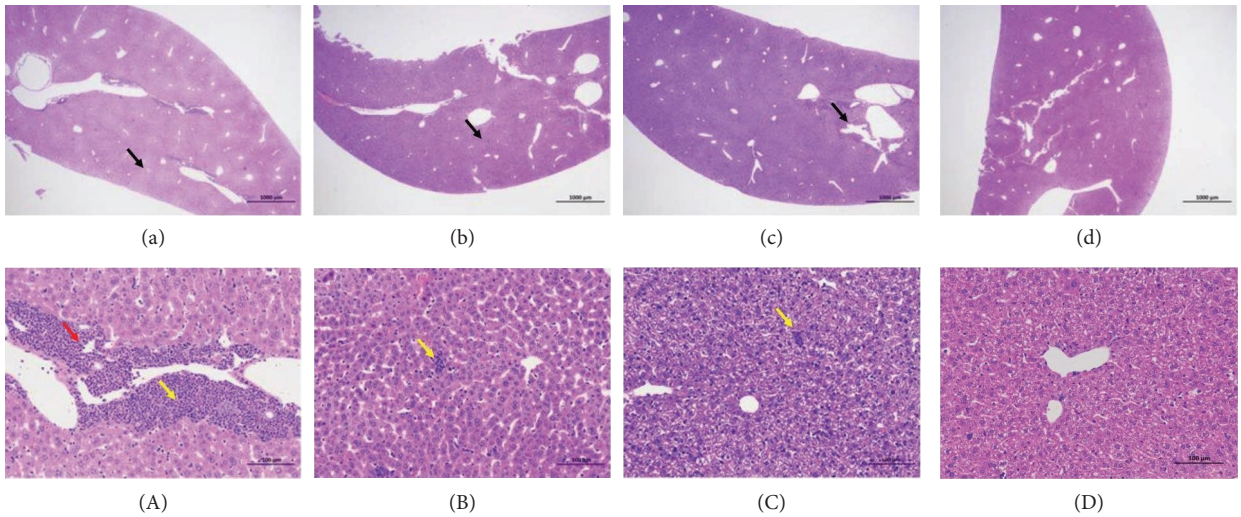

Figure 10: The effect of different treatment groups on mouse liver histology: (A) model group, (B) Corilagin high-dose group, (C) positive drug group, and (D) blank group (A–D: HE 200x; a–d: HE 20x).

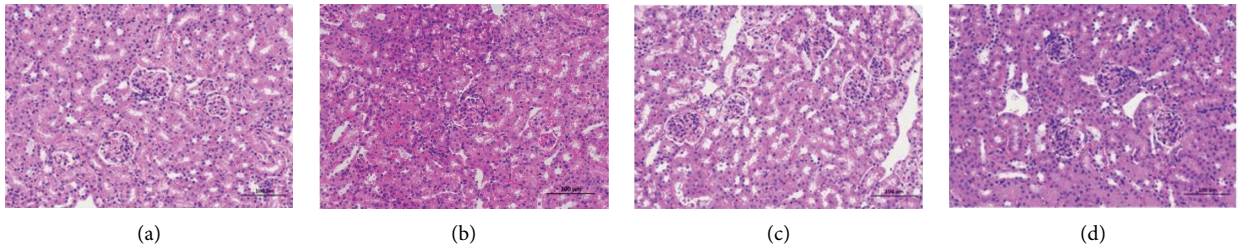

Figure 11: The effect of different treatment groups on mouse kidney histology (200x): (a) model group, (b) Corilagin high-dose group, (c) positive drug group, and (d) blank group.

high-dose Corilagin group and the positive drug group were significantly higher, whereas the content of IL-10 was significantly lower ($p < 0.05$).

3.10. Corilagin Modulates the Expression of Apoptosis-Related Genes in Tumor Tissues. Based on the result of network pharmacology, RT-PCR is used to verify and predict the

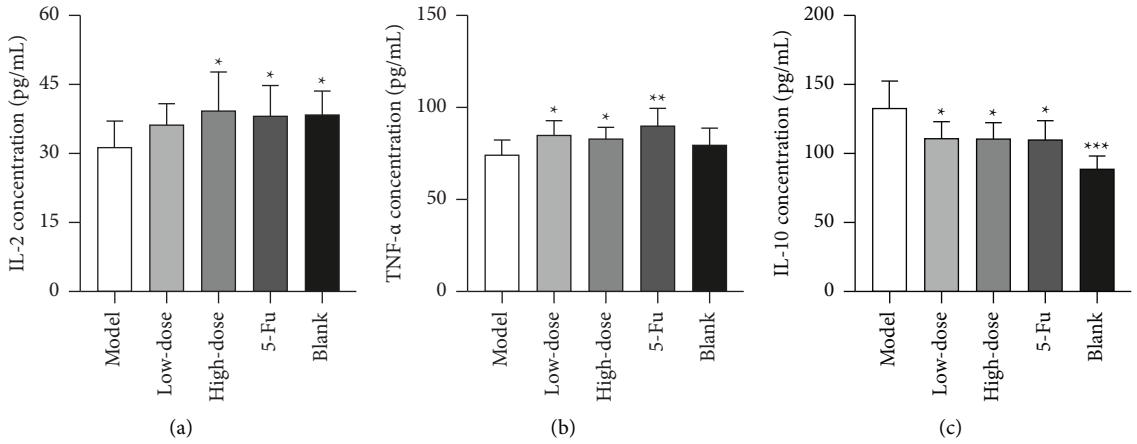

Figure 12: The effect of Corilagin on IL-2, TNF-α, and IL-10 in mouse serum: (a) IL-2, (b) TNF-α, and (c) IL-10 ($^{*}p < 0.05$, $^{**}p < 0.01$, and $^{***}p < 0.001$ vs. 0 μg/mL).

expression of target genes in PI3K/AKT and MAPK pathways. As shown in Figure 13, *Caspase3*, *Caspase9*, *Cytochrome C*, and *Bim* were significantly increased; the expression of *Bcl*-2 was significantly decreased ($p < 0.05$). This indicated that apoptosis-related genes were activated following treatment, leading to apoptosis of tumor tissues. The mRNA levels of *Egrf*, *Hras*, *Akt*, and *Erk* decreased significantly, and the mRNA expression of *FOXO3a*, *JNK*, and P38 increased ($p < 0.05$). Therefore, Corilagin may affect the glycolysis and apoptosis pathways of tumor tissues by downregulating the expression of *Egfr*, *Hras*, *Erk*, and *Akt* in tumor tissues and upregulating the expression of *JNK*, P38, and *Foxo3a*.

3.11. Changes in Protein Expression in Tumor Tissues. Results shown in Figure 14 demonstrated that the protein expression level of EGFR in tumor tissues was significantly lower after Corilagin treatment ($p < 0.05$), and AKT was higher after treatment compared with the model group. PI3K catalyzes Thr308 phosphorylation of AKT by binding to the AKT proteins and phosphatidylinositol-dependent I kinase containing PH domain. This suggests that Corilagin can affect the EGFR/AKT signaling pathway. Moreover, the expression of FOXO, a downstream target of the PI3K/AKT pathway, was increased, indicating that Corilagin regulated the PI3K/AKT pathway. The expression of Cyto C, Caspase3, and Caspase9 was increased significantly ($p < 0.01$), suggesting that Corilagin may induce tumor apoptosis. The protein expression levels of JNK and AMPK were significantly upregulated ($p < 0.05$). Corilagin may downregulate the protein expression of EGFR and AKT in tumor tissues, upregulate the protein expression of JNK, AMPK, FOXO, Cyto C, and CASPASE9, induce apoptosis of tumor tissues, and affect the growth of tumor tissues.

4. Discussion

Studies have shown that Corilagin has an inhibitory effect on a variety of cancers. Attar et al. [17] showed that Corilagin was antigastric cancer *in vitro* by inducing apoptosis,

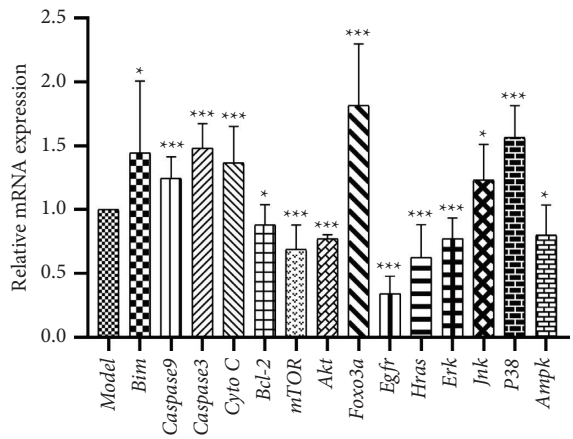

Figure 13: Expression levels of pathway related genes in tumor tissues. Expression levels of *Bim*, *Caspase 9*, *Caspase 3*, *Cyto C*, *Bcl-2*, *mTOR*, *Akt*, *Foxo3α*, *PI3k*, *Egfr*, *Hras*, *Erk*, *Jnk*, P38, and *Ampk* ($^{*}p < 0.05$ and $^{***}p < 0.001$ vs. model).

autophagy, and increasing reactive oxygen species generation; Wu et al. [18] isolated Corilagin from Phyllanthi Fructus and confirmed that it was antiesophageal cancer by activating mitochondrial and endoplasmic reticulum stress signaling pathways. The main purpose of this study was to verify the inhibitory effect of Corilagin on cervical cancer and to investigate its mechanism through *in vitro* and *in vivo* experiments.

Results of the CCK-8 assay in the present study showed that Corilagin significantly inhibited the proliferation of cervical cancer U14 cells of mice. Furthermore, it was found that Corilagin affected the cell growth by affecting the cell cycle distribution of U14 cells. Therefore, it was evident that Corilagin can significantly inhibit the growth of U14 tumor-bearing mice. The rate of tumor inhibition in the high-dose Corilagin group (30 mg/kg) was similar to that of the positive drug 5-FU (20 mg/kg). The results indicated that Corilagin could significantly inhibit the proliferation of the cervical cancer tissue. Organ coefficient and pathological section methods were used to detect drug toxicity of

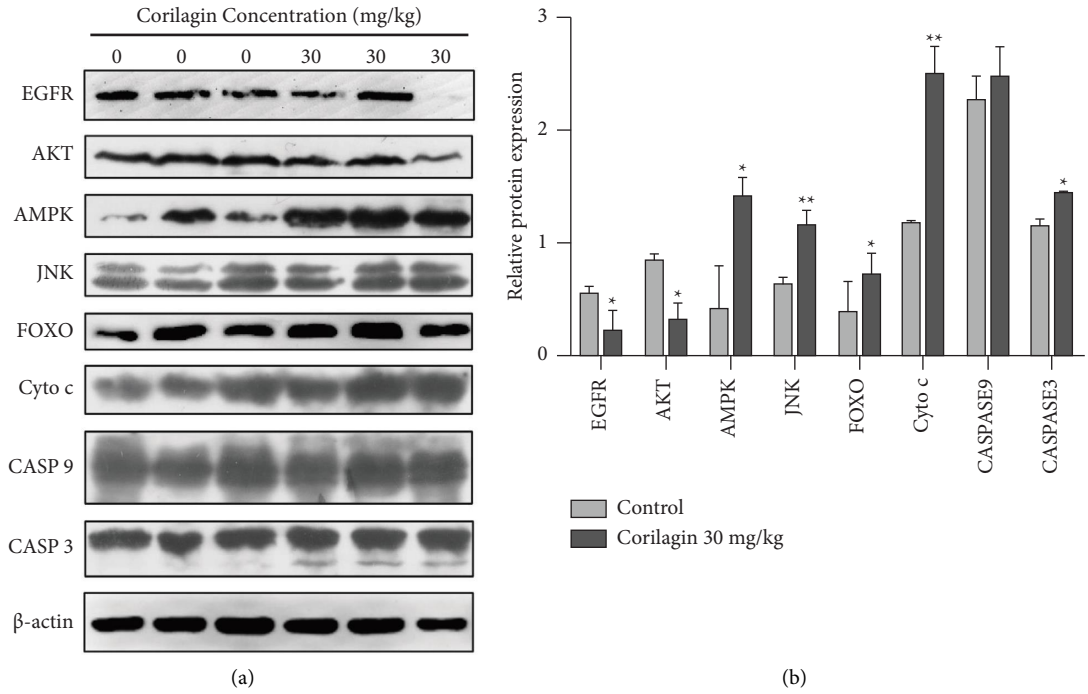

Figure 14: Changes in protein expression in tumor tissues: (a) changes of EGFR, AKT, AMPK, JNK, Cyto C, Caspase 9, and Caspase 3 in tumor tissues as determined by Western blot. (b) The average of EGFR, AKT, AMPK, JNK, Cyto C, Caspase 9, and Caspase 3 proteins band grayscale ($^{*}p < 0.05$ and $^{**}p < 0.01$ vs. model).

Corilagin in mice. In toxicology research, the organ gravimetric analysis is considered to be a vital indicator to detect whether a compound is harmful to the human body. Differences in organ weight are often compared with differences in body weight between different treatment groups, and the weight error can hence be eliminated by introducing organ coefficients [19]. Studies have shown that the coefficients of the liver, kidney, and spleen organs play a crucial reference role in prediction of a compound toxicity in the body [20]. In the present study, it was found that the organ coefficient was greater than that of the normal group, indicating that there were changes in the organ edema and congestion. In addition, it was evident that the organ coefficient was lower than that of the normal group, indicating organ atrophy or degenerative changes. Results of this study showed that Corilagin can significantly reduce the liver organ coefficient, but has no significant effect on the kidney organ coefficient. This indicated that Corilagin has a protective effect on the liver function, but may not have a significant toxic effect on the kidney tissues of mice. Furthermore, the results were basically consistent with those in the pathological sections of this study.

Subsequently, the mechanism of the anticervical cancer inhibits of Corilagin was studied. The results of network pharmacology indicated that Corilagin may achieve the effect of anticervical cancer by affecting PI3K/AKT, MAPK, and other signaling pathways. Furthermore, its mechanism of action may be associated with the signal pathway of apoptosis. Flow cytometry and TUNEL staining confirmed that Corilagin can induce apoptosis to affect the growth of the cervical cancer tissue.

The effects of Corilagin on mouse serum biochemical indices were studied through ELISA. It was found that helper T cells (Th cells) play a vital role in immune response of the body. Th cells have two subgroups: Th1 and Th2. Tumor progression is often accompanied by Th1/Th2 metastasis to Th2 [21], which is mainly because the imbalance of Th1/Th2 enables local T cells to escape the immune response to tumor tissues. Th1 cells mainly secrete cytokines such as TNF-β, TNF-α, and IL-2 which play a cytotoxic effect on killing cells. The IL-2 can not only stimulate NK cells to produce interferon, but also strengthen the function of Th1 cells and hence can strengthen the immune system of the body and induce tumor immune response [22]. TNF-α, or tumor necrosis factor-α, is not only a crucial regulator of the inflammatory response in the body, but can also form a complex with cell surface receptors or increase the adhesion of neutrophils to endothelial cells.

TNF-α has a direct cytotoxic effect on tumor cells [23]. Th2 cells mainly secrete cytokines such as IL-6 and IL-10. The cytokines IL-10 can reduce the proliferation of T cells, inhibit the antitumor immune response and the phagocytosis of monocytes/macrophages, and affect the growth proliferation as well as apoptosis of tumor cells. It has been found that the upregulation of IL-10 is closely related to the deterioration of cervical cancer [24]. This could be because the HPV oncogene protein E6 can affect the expression of IL-10 and the HPV escapes the detection of the immune system, which causes the occurrence of cervical cancer after continuous HPV infection [25].

The results of the current study showed that Corilagin can significantly increase the level of IL-2 and TNF-α in the

serum of mice. Furthermore, treatment with Corilagin reduced the level of IL-10, increased the level of Th1 cytokines, and reduced the level of Th2 cytokines. The finding indicates that Corilagin may enhance the antitumor immune response of the body by restoring the balance of the Th1/Th2 cell response and hence delay the progression of cervical cancer.

RT-PCR and Western blot analysis were used to validate the expression of target genes in network pharmacology prediction pathways. EGFR is an epidermal growth factor receptor that plays a significant role in growth and differentiation of tumors. Therefore, the production of a large number of cancer cells accompanied by high activation, overexpression, or signaling imbalance of EGFR is an upstream target of most tumor-related pathways. When EGFR is activated, EGFR ligands bind to the EGFR receptors, and the two undergo dimerization to stimulate RAS proteins in the downstream of the EGFR signaling pathway. These cause phosphorylation cascades, activate PI3K and MAPK signaling pathways, and affect the occurrence as well as development of tumors [26, 27]. A key downstream mediator of the PI3K signaling cascade is the serine/threonine kinase (AKT). This phosphorylates a variety of intracellular proteins to promote progression and activity of the cell cycle [28]. The MAPK subfamily includes ERK, JNK, and P38 that play key roles in the survival and apoptosis of various cancer cells through specific phosphorylation. Fluorescence quantitative results of the present study showed that after Corilagin treatment, the mRNA expressions of EGFR, and the RAS-related genes HRAS, AKT, and ERK were significantly decreased, whereas the mRNA expressions of JNK and P38 genes were increased after the treatment. Results of the Western blot assays showed that the expression levels of EGFR and p-Akt (Thr308) were significantly decreased, and the expression level of JNK was also significantly increased following the treatment of cells with Corilagin. This shows that Corilagin can trigger EGFR/RAS/AKT and EGFR/RAS/MAPK signaling pathways.

There are two pathways of apoptosis that are induced by complex cytotoxicity: death receptor pathway and mitochondrial pathway. The death receptor pathway mainly occurs through the binding of trimeric Fas to the receptor cytosolic domain and thereby triggering the Caspase cascade. Furthermore, the pathway relies on the interaction of the proteins in the Bcl-2 family to transport cytochrome C into the cytoplasm. After binding to apoptotic protease activator I, the Caspase-9 and Caspase-3 are activated, triggering a cascade reaction that causes apoptosis [29]. Therefore, it is evident that Bcl-2 family genes play a key role in the process of apoptosis. Anti-apoptotic proteins of Bcl-2 family include BCL-2 and BCL-XL, whereas the proapoptotic proteins include Bad and Bim [30].

The findings of RT-PCR showed that Corilagin treatment significantly decreased *Bcl-2* and significantly increased the mRNA expressions of *Caspase3*, *Caspase9, Cyto C,* and *Bim*. Results of the Western blot revealed that after treatment with Corilagin, the Caspase9 was significantly increased and this was an indication that Corilagin can induce cell apoptosis.

FOXO transcription factor is a downstream target for PI3K/AKT. AKT kinase-mediated phosphorylation regulates the transcriptional activity, whereas the cell activity is influenced by the transcriptional regulation of death receptor ligand and expression of Bim [31]. The phosphorylation of FOXO3A promotes the expression of downstream target genes, such as *Bim,* and the BH3 domain of Bim initiates the apoptotic cascade by binding BCL-2 and BCL-XL [32]. Furthermore, previous studies have found that tumor cells can induce apoptosis through AKT/FOXO3A/Bim signaling pathway [33]. The results on the levels of mRNA showed that the mRNA expression of *FOXO* and *Bim* was significantly upregulated. This suggests that Corilagin can induce apoptosis by activating the FOXO signaling pathway. Besides, this finding was same as the result that Corilagin promoted apoptosis of U14 cells *in vitro*.

In conclusion, it was evident that Corilagin can significantly upregulate mRNA expression off genes *Bim, Caspase3, Caspase9,* and *Cyto C* as well as Caspase9 protein expression. In addition, it was found that Corilagin can significantly downregulate the mRNA level of gene *Bcl-2* to activate AKT/FOXO3/Bim and JNK/P38 MAPK signaling pathways. Lastly, it was evident that the inhibition of AKT/HIF signaling pathway induces apoptosis in tumor tissues.

5. Conclusion

Network pharmacology can more accurately predict the anticervical cancer mechanism of Corilagin. The present study evidently showed that Corilagin can significantly inhibit the proliferation of U14 cells and affect the cell cycle and apoptosis *in vitro*. Results of *in vivo* experiments in the current study showed that Corilagin can significantly inhibit tumor growth, without causing significant toxicity to the body, enhance antitumor immune response, and induce tumor tissue apoptosis to achieve the effect of anticervical cancer in mice. However, there are no in-depth *in vivo* studies on the absorption, metabolism, and bioavailability of Corilagin and the pharmacokinetic process of Corilagin is still unclear. Therefore, there is a need for more in-depth research studies on the dosage, form, and pharmacokinetic process of Corilagin in animal bodies.

Data Availability

The datasets generated and/or analyzed during the current study are available in the PharmMapper (https://www.lilab-ecust.cn/pharmmapper/), SwissTargetPrediction (https://www.swisstargetprediction.ch/), Genecards (https://www.genecards.org/), OMIM (https://omim.org/), DisGeNET (https://www.disgenet.org/), STRING (https://www.string-db.org/), and DAVID (https://David.ncifcrf.gov/) repository.

Ethical Approval

This study was approved by the Research Ethics Committee of Wuhan Polytechnic University (No. WHPU20221023).

Disclosure

This article has been submitted as preprint according to the following link: https://quarxiv.authorea.com/doi/full/10.22541/au.167958238.82910186/v1 [32].

Conflicts of Interest

The authors declare that they have no conflicts of interest.

Acknowledgments

This work was supported by the Hubei Provincial Natural Science Foundation of China (2022CFB429) and Primary Research & Development Plan of Hubei Province (2022BBA0023).

Supplementary Materials

Supplement materials Table S1: primer sequence. Supplement materials Table S2: the IC_{50} value of the inhibitory effect of Corilagin and 5-FU on U14 cell proliferation at 24 h and 48 h. Supplement materials Table S3: the effects of Corilagin and 5-FU on tumor weight in mice. Supplementary Figure S1: the role of key targets and other targets in the tumor signal pathway diagram. (*Supplementary Materials*)

References

[1] F. Bray, J. Ferlay, I. Soerjomataram, R. L. Siegel, L. A. Torre, and A. Jemal, "Global cancer statistics 2018: GLOBOCAN estimates of incidence and mortality worldwide for 36 cancers in 185 countries," *CA: A Cancer Journal for Clinicians*, vol. 68, no. 6, pp. 394–424, 2018.

[2] L. Cao, H. Wen, Z. Feng, X. Han, and X. Wu, "Distinctive clinicopathologic characteristics and prognosis for different histologic subtypes of early cervical cancer," *International Journal of Gynecological Cancer*, vol. 29, no. 8, pp. 1244–1251, 2019.

[3] M. Arbyn, E. Weiderpass, L. Bruni et al., "Estimates of incidence and mortality of cervical cancer in 2018: a worldwide analysis," *Lancet Global Health*, vol. 8, no. 2, pp. e191–e203, 2020.

[4] D. B. Longley, D. P. Harkin, and P. G. Johnston, "5-Fluorouracil: mechanisms of action and clinical strategies," *Nature Reviews Cancer*, vol. 3, no. 5, pp. 330–338, 2003.

[5] X. Li, Y. Deng, Z. Zheng et al., "Corilagin, a promising medicinal herbal agent," *Biomedicine & Pharmacotherapy*, vol. 99, pp. 43–50, 2018.

[6] S. G. Yeo, J. H. Song, E. H. Hong et al., "Antiviral effects of Phyllanthus urinaria containing Corilagin against human enterovirus 71 and coxsackievirus A16 in vitro," *Archives of Pharmacal Research*, vol. 38, no. 2, pp. 193–202, 2015.

[7] X. Qin, J. Liu, D. Pan, W. Ma, P. Cheng, and F. Jin, "Corilagin induces human glioblastoma U251 cell apoptosis by impeding activity of (Immuno)proteasome," *Oncology Reports*, vol. 45, no. 4, p. 34, 2021.

[8] M. Wu, Y. Jiang, J. Wang et al., "The effect and mechanism of Corilagin from Euryale ferox salisb shell on LPS-induced inflammation in Raw264.7 cells," *Foods*, vol. 12, no. 5, p. 979, 2023.

[9] A. Gupta, A. K. Singh, R. Kumar et al., "Corilagin in cancer: a critical evaluation of anticancer activities and molecular mechanisms," *Molecules*, vol. 24, p. 3399, 2019.

[10] L. Zhao, S. L. Zhang, J. Y. Tao et al., "Preliminary exploration on anti-inflammatory mechanism of Corilagin (beta-1-O-galloyl-3,6-(R)-hexahydroxydiphenoyl-D-glucose) in vitro," *International Immunopharmacology*, vol. 8, no. 7, pp. 1059–1064, 2008.

[11] J. S. Londhe, T. P. Devasagayam, L. Y. Foo, and S. S. Ghaskadbi, "Antioxidant activity of some polyphenol constituents of the medicinal plant Phyllanthus amarus linn," *Redox Report*, vol. 13, no. 5, pp. 199–207, 2008.

[12] I. Berdowska, M. Matusiewicz, and I. Fecka, "Punicalagin in cancer prevention-via signaling pathways targeting," *Nutrients*, vol. 13, no. 8, p. 2733, 2021.

[13] A. V. Vaseva and M. E. Yohe, "Targeting RAS in pediatric cancer:is it becoming a reality?" *Current Opinion in Pediatrics*, vol. 32, no. 1, pp. 48–56, 2020.

[14] A. Kortholt, P. Bolourani, H. Rehmann et al., "A rap/phosphatidylinositol 3-kinase pathway controls pseudopod formation," *Molecular Biology of the Cell*, vol. 21, no. 6, pp. 936–945, 2010.

[15] M. Ingham and G. K. Schwartz, "Cell-cycle therapeutics come of age," *Journal of Clinical Oncology*, vol. 35, no. 25, pp. 2949–2959, 2017.

[16] Y. Ming, Z. Zheng, L. Chen et al., "Corilagin inhibits hepatocellular carcinoma cell proliferation by inducing G2/M phase arrest," *Cell Biology International*, vol. 37, no. 10, pp. 1046–1054, 2013.

[17] R. Attar, Z. B. Cincin, E. S. Bireller, and B. Cakmakoglu, "Apoptotic and genomic effects of Corilagin on SKOV3 ovarian cancer cell line," *OncoTargets and Therapy*, vol. 10, pp. 1941–1946, 2017.

[18] C. Wu, H. Huang, H. Y. Choi et al., "Anti-esophageal cancer effect of Corilagin extracted from Phmllanthi Fructus via the mitochondrial and endoplasmic reticulum stress pathways," *Journal of Ethnopharmacology*, vol. 269, 2021.

[19] R. Zhang, L. Zhang, D. Jiang et al., "Mouse organ coefficient and abnormal sperm rate analysis with exposure to tap water and source water in nanjing reach of yangtze river," *Ecotoxicology*, vol. 23, no. 4, pp. 641–646, 2014.

[20] C. C. Gould, "Solidarity and the problem of structural injustice in healthcare," *Bioethics*, vol. 32, no. 9, pp. 541–552, 2018.

[21] Q. Shang, X. Yu, Q. Sun, H. Li, C. Sun, and L. Liu, "Polysaccharides regulate Th1/Th2 balance: a new strategy for tumor immunotherapy," *Biomedicine & Pharmacotherapy*, vol. 170, 2024.

[22] L. Chen, J. Pan, X. Li, Y. Zhou, Q. Meng, and Q. Wang, "Endopolysaccharide of phellinus igniarius exhibited anti-tumor effect through enhancement of cell mediated immunity," *International Immunopharmacology*, vol. 11, no. 2, pp. 255–259, 2011.

[23] B. L. Salomon, M. Leclerc, J. Tosello, E. Ronin, E. Piaggio, and J. L. Cohen, "Tumor necrosis factor α and regulatory T cells in oncoimmunology," *Frontiers in Immunology*, vol. 9, p. 444, 2018.

[24] K. Torres-Poveda, M. Bahena-Roman, C. Madrid-Gonzalez et al., "Role of IL-10 and TGF-β1 in local immunosuppression in HPV-associated cervical neoplasia," *World Journal of Clinical Oncology*, vol. 5, no. 4, pp. 753–763, 2014.

[25] I. Arany, K. G. Grattendick, and S. K. Tyring, "Interleukin-10 induces transcription of the early promoter of human papillomavirus type 16 (HPV16) through the 5'-segment of the

upstream regulatory region (URR)," *Antiviral Research*, vol. 55, no. 2, pp. 331–339, 2002.

[26] C. Y. Chuang, W. W. Sung, L. Wang et al., "Differential impact of IL-10 expression on survival and relapse between HPV16-positive and-negative oral squamous cell carcinomas-negative oral squamous cell carcinomas," *PLoS One*, vol. 7, no. 10, 2012.

[27] S. Kasper, H. Reis, S. Ziegler et al., "Molecular dissection of effector mechanisms of RAS-mediated resistance to anti-EGFR antibody therapy," *Oncotarget*, vol. 8, no. 28, pp. 45898–45917, 2017.

[28] R. Roskoski Jr., "The ErbB/HER receptor protein-tyrosine kinases and cancer," *Biochemical and Biophysical Research Communications*, vol. 319, no. 1, pp. 1–11, 2004.

[29] H. I. Lin, Y. J. Lee, B. F. Chen et al., "Involvement of Bcl-2 family, cytochrome and caspase 3 in induction of apoptosis by beauvericin in human non-small cell lung cancer cells," *Cancer Letters*, vol. 230, no. 2, pp. 248–259, 2005.

[30] D. Lama and R. Sankararamakrishnan, "Anti-apoptotic bcl-XL protein in complex with BH3 peptides of pro-apoptotic bak, Bad, and Bim proteins: comparative molecular dynamics simulations," *Proteins: Structure, Function, and Bioinformatics*, vol. 73, no. 2, pp. 492–514, 2008.

[31] H. Guan, L. Song, J. Cai et al., "Sphingosine kinase 1 regulates the akt/FOXO3a/bim pathway and contributes to apoptosis resistance in glioma cells," *PLoS One*, vol. 6, no. 5, p. e19946, 2011.

[32] A. Aranovich, Q. Liu, T. Collins et al., "Differences in the mechanisms of proapoptotic BH3 proteins binding to bcl-XL and bcl-2 quantified in live MCF-7 cells," *Molecular Cell*, vol. 45, no. 6, pp. 754–763, 2012.

[33] G. Sharma, S. Kar, S. Palit, and P. K. Das, "18β-glycyrrhetinic acid induces apoptosis through modulation of Akt/FOXO3a/Bim pathway in human breast cancer MCF-7 cells," *Journal of Cellular Physiology*, vol. 227, no. 5, pp. 1923–1931, 2012.